System Concepts for Cycle Ambiguity Resolution and Verification for Aircraft Carrier Landings

Boris Pervan and Fang-Cheng Chan

Department of Mechanical, Materials, and Aerospace Engineering, Illinois Institute of Technology

Demoz Gebre-Egziabher, Sam Pullen, Michael Koenig, Ung-Souk Kim, and Per Enge

Department of Aeronautics and Astronautics, Stanford University

ABSTRACT

The Shipboard-Relative GPS (SRGPS) variant of the Joint Precision Approach and Landing System (JPALS) is being developed with the ultimate goal of providing navigation to support automatic shipboard landings in zero-visibility conditions. At present, the required vertical protection level for the navigation system is 1.1 m, with an associated integrity risk of approximately 10^{-7}. Furthermore, it is desired that the integrity requirements be satisfied with a system availability of at least 99.85%. Because of the stringent nature of these requirements, differential carrier phase solutions are being pursued. In this context, this paper gives a detailed analysis of the fault-free (H0) integrity of SRGPS and introduces a number of relevant shipboard integrity monitoring concepts for fault detection. The sensitivity of SRGPS performance is quantified with respect to raw code and carrier measurement quality (standard deviations and time constants), spatial decorrelation of ionospheric and tropospheric errors, and broadcast service radius (which limits airborne filter duration). It is shown that while all of these elements do influence SRGPS performance, navigation system availability is most significantly affected by raw code (pseudorange) and carrier measurement error. The tradeoff between measurement error requirements and broadcast service radius is explicitly quantified.

INTRODUCTION

Shipboard-Relative GPS (SRGPS) is an architectural variant of the Joint Precision Approach and Landing System (JPALS) which is being developed to provide high accuracy and high integrity navigation for automatic shipboard landings. The required navigation system vertical accuracy is currently envisioned to be on the order of 0.3 m, and the vertical protection level is 1.1 m, with an associated integrity risk of approximately 10^{-7}. In order to provide such navigation performance with adequate system availability (at least 99.85%), differential carrier phase solutions are presently being pursued. [1]

The full availability of both the L1 and L2 GPS signals for this military application is tempered by the simultaneous need to provide redundancy in the event of hostile jamming or interference. In this respect, although dual-frequency architectures may be acceptable for SRGPS, a single-frequency carrier phase solution would be preferable. In addition, controlled reception pattern (phased array) shipboard antennas will be implemented in SRGPS to provide superior performance in a jamming environment and to mitigate multipath. These antennas can be expected to benefit SRGPS performance by providing exceptionally precise code and carrier measurements for satellites at all elevations. [2]

The use of differential carrier phase for precise navigation is contingent upon the successful estimation or resolution of cycle ambiguities. While it is understood that fixed-integer implementations will provide better accuracy than floating ambiguity implementations, the integrity of cycle resolution process must be ensured. In the most general sense, cycle resolution integrity will be a function of the quality of the raw code and carrier measurements, satellite geometry, and filter duration. For example, a large service volume can potentially provide sufficient time for averaging of noisy measurements, and also for satellite motion, to improve cycle ambiguity observability. In this case, however, the spatial decorrelation of carrier phase measurement errors (over the resulting long baselines) must be carefully accounted for.

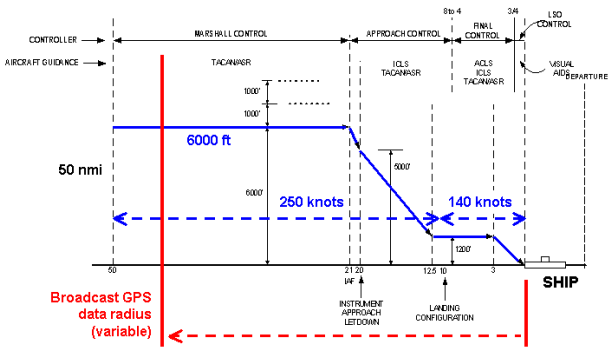

Figure 1: Nominal Airplane Approach Model

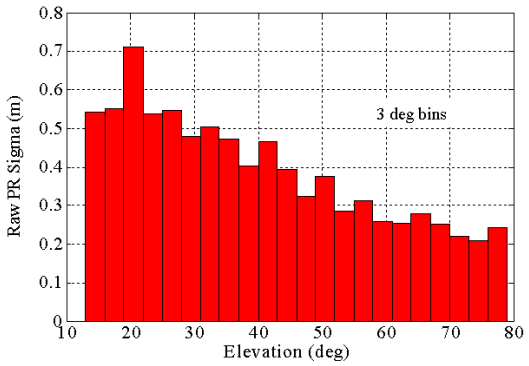

Figure 2: SRGPS Shipboard Pseudorange Measurement Error

It is intuitively clear that the performance of carrier-phase-based DGPS (for both floating and fixed ambiguity implementations) will be better if:

- Dual frequency measurements are used (instead of L1 alone).
- GPS data broadcast radius is large (providing longer filtering time and more satellite motion).
- High performance antennas are used (smaller raw code and carrier measurement error).

While these observations are all qualitatively true, we seek *quantitative* design guidelines and tradeoffs applicable to SRGPS. Some specific questions which require quantitative answers include:

- Given a specified GPS data broadcast radius (which defines maximum filter duration), how small should raw measurement errors be to ensure adequate SRGPS availability? The answer may be interpreted as a derived system requirement on antenna /receiver performance.
- To what other errors sources or parameters is SRGPS performance most sensitive? (Some examples include multipath time constant, residual tropospheric error decorrelation, and ionospheric spatial gradient.)
- Can we quantify the benefit in fixing integers (relative to a floating implementation), given that the probability of incorrect integer fix must be consistent with integrity requirements? To what extent does integer fixing allow relaxation of requirements on antenna quality and/or GPS data broadcast radius?
- How do the answers to the questions above differ for single and dual frequency cases?

In this paper we seek to answer these questions to provide a basis for defining necessary conditions (i.e., derived requirements) for adequate fault-free availability of SRGPS navigation. In addition, a number of relevant shipboard integrity monitoring concepts for fault detection are introduced.

ANALYSIS METHODOLOGY

To explore the sensitivity of SRGPS performance to variations in system and measurement error characteristics we used a *covariance analysis* methodology. A nominal fixed-wing (airplane) approach model, illustrated in Figure 1, was assumed in this analysis [3], [4]. The GPS data broadcast radius, also indicated in the figure, was treated as a parameter. Within the broadcast radius, code and carrier measurements from the shipboard reference receiver(s) were assumed available for use at the aircraft. The nominal DO-229A (WAAS MOPS) [5] GPS satellite constellation, a Central Pacific ship location (22 deg N, 158 deg W), and a satellite elevation mask of 7.5 deg were used in the analysis. Both single and dual frequency implementations were considered in this work. The measurement error models used in the covariance analysis as well as details regarding the floating and fixed cycle ambiguity implementations are described below.

Multipath/Receiver Noise Error Model

Both code and carrier errors were modeled as First Order Gauss-Markov Random Processes (GMRPs). Independent GMRPs were assumed for code and carrier for each frequency and for each satellite. The associated GMRP standard deviations and time constants were treated as parameters which were varied in the analysis to quantify the effect of receiver/antenna quality on overall SRGPS performance. A 'nominal' set of model parameters, used as a reference for sensitivity analysis, is defined below

- Time constant: $\tau = 40$ sec
- P(Y) Code: $\sigma_{PR} = 0.3$ m
- Carrier: $\sigma_{\phi} = 1$ cm

The nominal standard deviations listed correspond to single difference measurement errors for both L1 and L2 measurements for all satellites, independent of elevation. The nominal time constant applies to all measurement errors. For comparison, Figure 2 shows a histogram of standard deviation of raw code measurement error obtained from shipboard measurement data collected during SRGPS flight demonstration trials in April 2001 (using an EMAGR reference receiver and choke ring antenna). [6] In the creation of the histogram, some low elevation data at discrete azimuths was culled to exclude effects of masking due to ship structure. The observed measurement error time constants varied widely for individual satellites from about 10 to 300 sec.

Residual Tropospheric Decorrelation

Residual differential tropospheric error (i.e., the ranging error remaining after tropospheric correction) was modeled using the Local Area Augmentation System (LAAS) tropospheric error model: [7]

$$\varepsilon_T(i,k) = \Delta n \cdot \frac{h_0\left[1-\exp\left(-h(k)/h_0\right)\right]}{\sqrt{0.002+\sin^2 E(i,k)}} \qquad (1)$$

where ε_T is the tropospheric error, Δn is the error in knowledge of local index of refraction, h_0 is the troposphere scale height, h is the altitude of the airplane, E is satellite elevation, and i and k are satellite and time indices, respectively.

The local refraction index error Δn was included as a *state* in the covariance analysis. At aircraft approach initiation, the uncertainty in knowledge of the refraction error state was defined by $\Delta n \sim N(0,\ 10^{-6}\sigma_N)$. For a nominal error model, we assumed $\sigma_N = 10$ and $h_0 = 7000$ m, but these parameters were varied in the sensitivity analysis.

Ionospheric Spatial Gradient

The differential ranging error due to ionospheric spatial gradient was also modeled in this analysis using the associated LAAS model: [7]

$$\varepsilon_I(i,k) = VIG_i \cdot x(k) \Bigg/ \sqrt{1+\left(\frac{R_e\cos E(i,k)}{R_e+h_I}\right)^2} \qquad (2)$$

where ε_I is the L1 ionospheric error (negative for carrier), VIG is the vertical ionospheric gradient, h_I is the ionospheric shell height (350 km), R_E is the earth radius, and x is the distance of the airplane from the ship. (E, i and k are as defined earlier.)

In the covariance analysis, *an independent VIG state* was included for each satellite. At aircraft approach initiation, the uncertainty in knowledge of each *VIG* state was defined by $VIG_i \sim N(0,\ \sigma_{VIG})$. For a nominal error model, we assumed $\sigma_{VIG} = 1$ mm/km, but this parameter was also varied in the sensitivity analysis.

Floating and Fixed Integer Implementation Models

During each simulated approach, both aircraft and satellite motion were modeled. The state covariance matrix (including floating cycle ambiguity, position, and error model states) was propagated in time during the approach. For *floating implementation* results, only the time history vertical position error standard deviation σ_{vert} (a direct output of the covariance propagation) was of interest. The basic performance criteria used in this analysis was the Vertical Protection Level under fault-free conditions (VPL_{H0}), defined by

$$\begin{aligned} &\text{Prob}\left\{\left|\hat{x}_{vert}-x_{vert}\right| > VPL_{H0}\right\} = 10^{-7} \\ &\Rightarrow \qquad VPL_{H0} = 5.33\,\sigma_{vert} \end{aligned} \qquad (3)$$

It is noted that in this initial analysis, we have allocated the total allowable navigation integrity risk (10^{-7}) entirely to the fault-free case. For navigation availability it is required that $VPL_{H0} < VAL$, where VAL is the specified Vertical Alert Limit (1.1 m). Overall fault-free service availability (A_{FF}) was defined as:

$$A_{FF} = \text{Prob}\left\{VPL_{H0} < VAL\right\}. \qquad (4)$$

For *fixed-integer implementations*, a correct fix (CF) of the cycle ambiguities, or some subset linear combination of cycle ambiguities, will improve positioning performance: $\sigma_{vert|CF} < \sigma_{vert}$. Obviously, for a fixed integer implementation it is desired that the probability of incorrect fix (P_{IF}) be small. In mathematical terms, the associated VPL_{H0} is defined by:

$$\begin{aligned} &\text{Prob}\left\{\left|\hat{x}_{vert}-x_{vert}\right| > VPL_{H0}\,\middle|\,CF\right\}\cdot(1-P_{IF}) \\ &+\ \text{Prob}\left\{\left|\hat{x}_{vert}-x_{vert}\right| > VPL_{H0}\,\middle|\,IF\right\}\cdot P_{IF} = 10^{-7} \end{aligned} \qquad (5)$$

Given an incorrect fix, it is assumed that the resulting position error will generally be large:

$$\text{Prob}\left\{\left|\hat{x}_{vert}-x_{vert}\right| > VPL_{H0}\,\middle|\,IF\right\} \approx 1 \qquad (6)$$

Substituting (6) into (5), we obtain

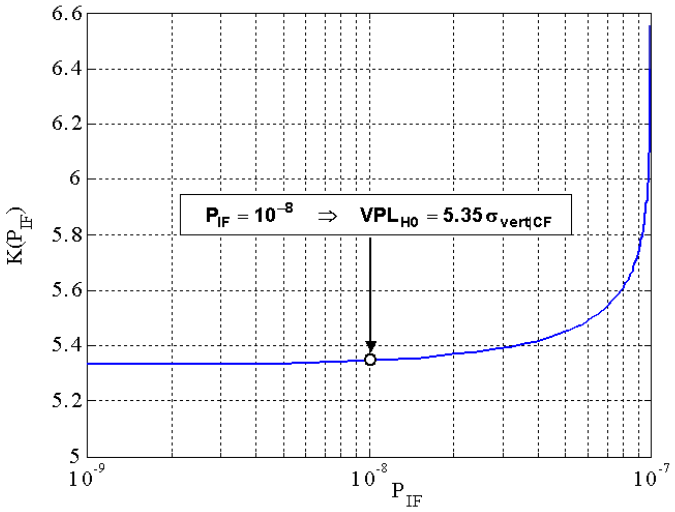

Figure 3: Integrity Multiplier (k) as a Function of P_{IF}

$$\text{Prob}\left\{\left|\hat{x}_{vert} - x_{vert}\right| > VPL_{H0} \,\middle|\, CF\right\} = \frac{10^{-7} - P_{IF}}{1 - P_{IF}} \qquad (7)$$

so that

$$VPL_{H0} = k(P_{IF}) \cdot \sigma_{vert\,|\,CF} \,. \qquad (8)$$

The integrity multiplier (k) in equation (8) is plotted as a function of P_{IF} in Figure 3. For very small P_{IF}, the integrity multiplier approaches 5.33, the value in equation (3). However, as P_{IF} approaches 10^{-7}, the integrity multiplier, and hence VPL_{H0}, grows very large. For this analysis, we imposed a reasonable, intermediate requirement on the 'fixed' implementation: $P_{IF} < 10^{-8}$. In this case,

$$VPL_{H0} = 5.35\,\sigma_{vert\,|\,CF} \,. \qquad (9)$$

The fixed integer implementation model used in this analysis was Teunissen's 'Integer Bootstrapping' algorithm with LAMDA cycle ambiguity decorrelation. [8] The Integer Bootstrapping implementation is a successive rounding approach which has two significant benefits for our application:

- The probability of correct fix (P_{CF}) can be computed directly.
- Fixing can be restricted to only those cycle ambiguities (or linear combinations thereof) which have high P_{CF}.

At a given time during the airplane approach, the covariance matrix on cycle ambiguity estimate error was

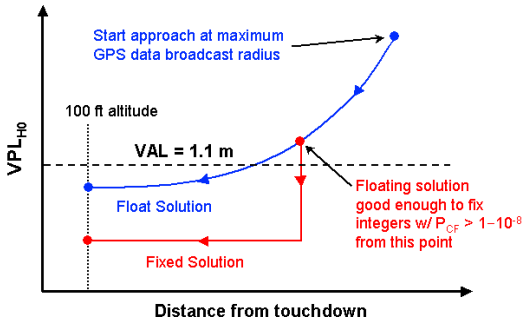

Figure 4: Results for a Single Hypothetical Approach

obtained from floating covariance propagation. It was then determined whether for some (or all) linear combinations of cycle ambiguities $P_{CF} > 1-10^{-8}$. If so, the position error covariance was updated assuming the associated integers were precisely known. Otherwise, the (floating) covariance matrix was propagated until the next measurement update.

An illustrative example of a hypothetical airplane approach result is shown in Figure 4. The approach begins at the specified GPS data broadcast radius (at the far right in the figure). As time passes, the aircraft approaches the ship ('distance from touchdown' gets smaller) and the combined effect of filtering and satellite motion will cause σ_{vert} (floating), and therefore VPL_{H0}, to become smaller. At a certain point during the approach the probability of correct fix may become larger than the minimum required. From this point on, a fixed solution is possible.

To consolidate the results from a large number of simulated approaches (associated with different satellite geometries and SRGPS parameter values) in a relatively compact way, most results will be presented as illustrated in the right-hand plot in Figure 5. Here, a single curve is used to define the variation in VPL_{H0} at 100 ft altitude with GPS data broadcast radius (DBR), for a given satellite geometry. The satellite geometry is matched (for all of the approaches used to generate the curve) at the 100 ft altitude point; thus, as DBR increases the final geometry is the same, but there exists a longer prior exposure time for satellite motion and filtering. In this way, the results for many satellite geometries (many such curves) can be presented on a single plot. The quantitative results for a single representative satellite geometry, using the nominal error models defined earlier, are shown in are shown in Figure 6.

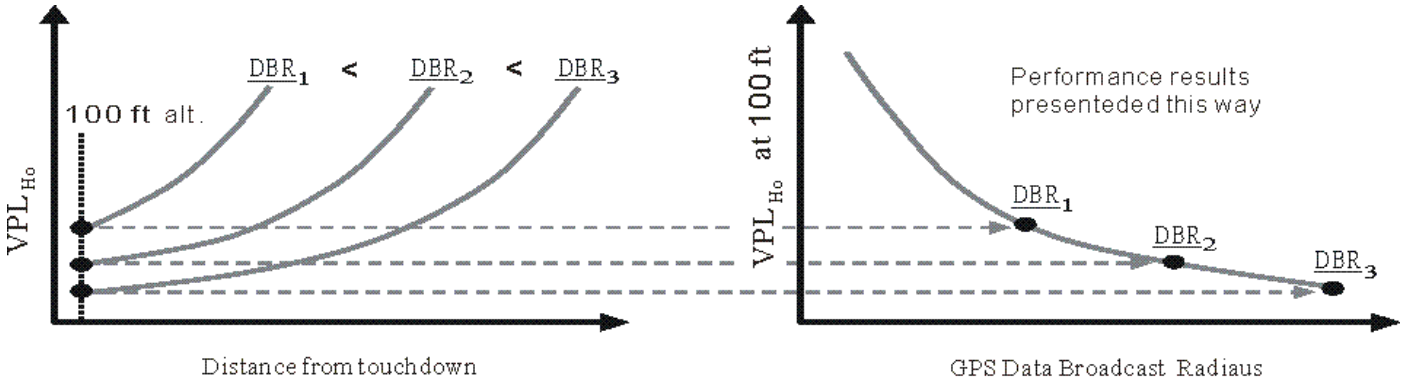

Figure 5: Format of Plotted Results

PARAMETER SENSITIVITY

The relative sensitivity of dual-frequency SRGPS performance to the error model parameters was explored by varying each parameter individually from its nominal reference value. In the results which follow, the satellite geometry used is the same as that used to generate the (nominal) results in Figure 6. In each sensitivity plot, the nominal (Figure 6) result is also shown for direct comparison.

Figure 7 shows the sensitivity of performance to a 50% increase in σ_{PR}. It is clear that the performance of the floating implementation is affected for all values of *DBR*. This result is intuitively reasonable because for any given filter duration (which is defined by *DBR*) a decrease in raw pseudorange error will always result in statistically better estimates of vertical position and floating cycle ambiguities. Integer fixing is still possible, but the minimum *DBR* required to ensure integrity is larger.

Figure 8 shows that a 50% increase in σ_ϕ (carrier phase measurement error) primarily affects floating implementation performance when *DBR* is large. In this case, the benefits of satellite motion to cycle ambiguity observability are realized through carrier phase measurements, and are therefore sensitive to σ_ϕ, but the effects are only significant for longer exposure times (larger *DBR*). In contrast, for the fixed integer implementation, the effect is more significant in the sense that a larger *DBR* (more averaging) is required to ensure that integers can be fixed with the required integrity.

The effect of a 50% increase in measurement error time constant is shown in Figure 9. Performance is generally degraded, although to a somewhat lesser extent, for small *DBR*. In this case, the performance is dominated directly by σ_{PR} (raw code error) because little time is available for filtering, regardless of the measurement error time constant.

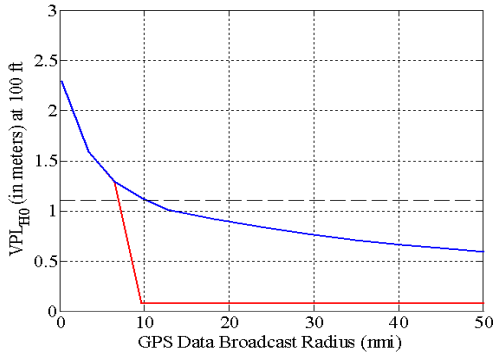

Figure 6: Results for a Typical Approach Using 'Nominal' Error Model

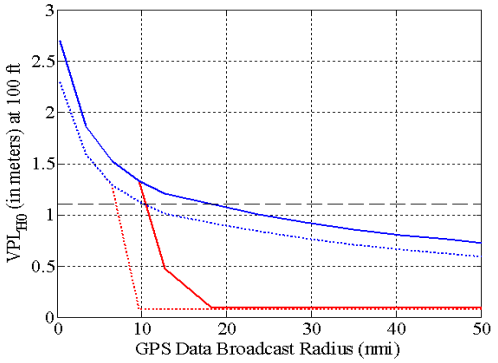

Figure 7: Sensitivity to σ_{PR} (50% Increase)

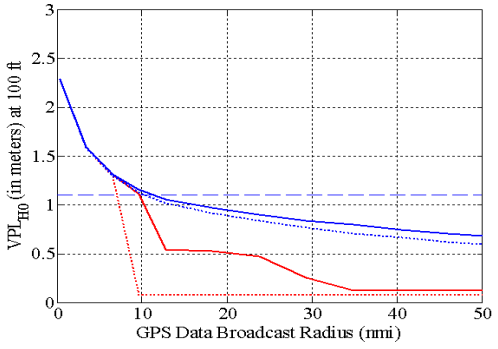

Figure 8: Sensitivity to σ_ϕ (50% Increase)

Figure 10 shows the effect of variation of ionospheric

gradient parameter (σ_{VIG}). It is evident that there is relatively small impact on performance due to a 50% variation in ionospheric gradient uncertainty for any value of *DBR*. It was also determined that the performance is similarly insensitive to variations in tropospheric error parameters σ_N and h_0. While these observations may be true at face value, it should again be noted that *only the vertical performance at 100 ft altitude* is represented on the plots. In contrast, Figure 11 shows the *time history* of VPL_{H0} during the approach (using the same satellite geometry) with *DBR* = 50 nmi, given an increased σ_{VIG}. The figure shows that performance *during the approach* is affected by a variation in the ionospheric error parameter, but as the aircraft approaches the ship, the net impact gradually diminishes. (The same is true for the variations in tropospheric error.) It must also be noted that these results, in particular the lack of ionospheric sensitivity, apply to *dual-frequency* SRGPS implementations only. As will be seen shortly, *single-frequency* performance is strongly affected by ionospheric spatial gradient.

Assuming that a *small DBR* is most likely desirable from data link design perspective, the sensitivity results suggest that dual frequency SRGPS performance is most strongly affected by raw pseudorange error (σ_{PR}) for the floating case, and is also is influenced by σ_ϕ and τ for the fixed implementation. In addition, it is also worth noting that an SRGPS solution which relies on a relatively small *DBR* will be implicitly more robust to spatial decorrelation error model assumptions.

FAULT-FREE AVAILABILITY

We next evaluated single and dual-frequency SRGPS performance over an entire day of satellite geometries. The availability results presented here were based on fault-free (H0) performance with a full constellation (no satellite outages). In this sense the results were interpreted as upper bounds on availability given the specified error models. The sensitivity of system availability to σ_{PR} was of particular interest.

Dual Frequency Availability

The covariance analysis results for a full day of satellite geometries (using the nominal error models) are shown in Figures 12 and 13 for floating and fixed integer implementations, respectively. It is clear that even with the constraint $P_{IF} < 10^{-8}$, the fixed-integer performance is superior to the floating implementation in the sense that much smaller *DBR* values are required to achieve sub-*VAL* performance.

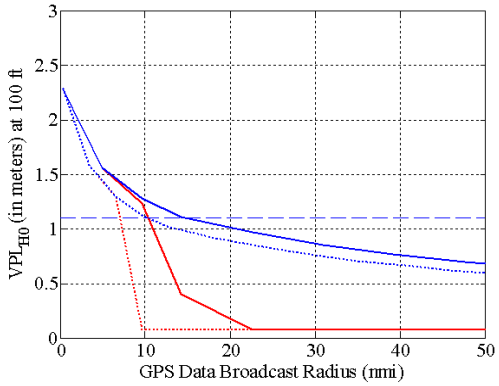

Figure 9: Sensitivity to τ (50% Increase)

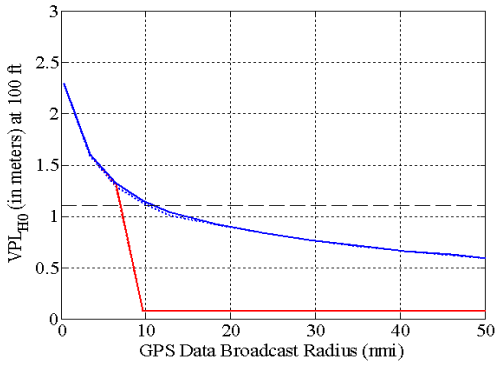

Figure 10: Sensitivity to σ_{VIG} (50% Increase)

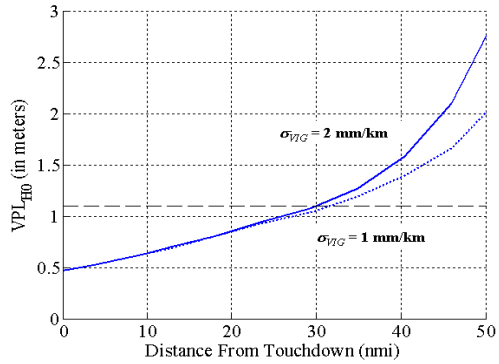

Figure 11: Sensitivity of VPL_{H0} During Approach to σ_{VIG}

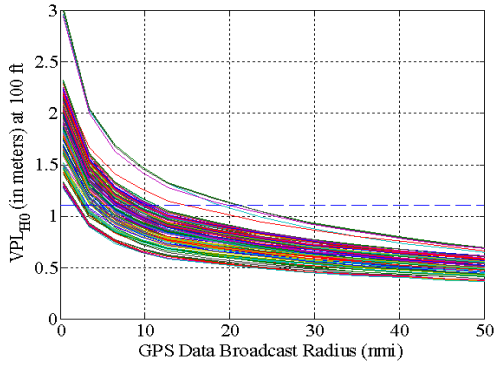

Figure 12: Full Day Results: Dual Frequency Floating Implementation

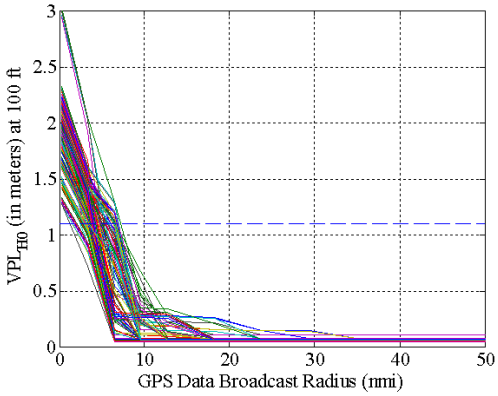

Figure 13: Full Day Results: Dual Frequency Fixed Implementation

Figure 14 shows full-constellation H0 'unavailability' results ($1-A_{FF}$) for values of σ_{PR} equal to 10, 30, and 50 cm and measurement error time constants of 40 sec and 2 min. It is obvious that availability is a strong function σ_{PR}. This is true in the most direct sense because as σ_{PR} is lowered, poorer geometries become acceptable. In addition, however, it is also true that as σ_{PR} is lowered, positioning performance near the ship is less dependent on prior filtering during the approach. For this reason lower *DBR*s can be supported, and sensitivity to measurement error time constant decreases significantly. As noted above, the ability to achieve good availability with a small *DBR* also provides increased robustness against ionospheric and tropospheric decorrelation model errors. For good (full constellation) H0 availability with DBR = 10 nmi and weak sensitivity to error time constant it is necessary that σ_{PR} be smaller than roughly 20 cm. Note that when satellite outages are considered, a more stringent requirement will undoubtedly result. SRGPS results with satellite outages will be published in a future paper.

Single Frequency Availability

The full-day floating and fixed-integer results for a single frequency SRGPS implementation (using the nominal error model) are shown in Figures 15 and 16. It is immediately clear that the performance here is much worse than that seen for the dual frequency case. Furthermore, the use of a fixed integer implementation provides relatively little benefit. The primary reason for the poor performance exhibited is that the single-frequency implementation is affected much more significantly by ionospheric gradient. For comparison, Figures 17 and 18 show much better performance when $\sigma_{VIG} = 0$. It is nevertheless clear that, even in this idealized case, integer fixing provides relatively little improvement in availability relative to a floating implementation: When integer fixing is possible with P_{IF}

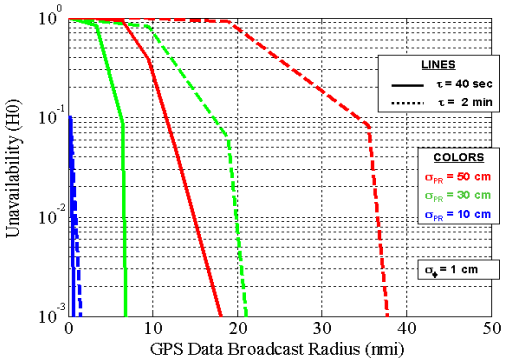

Figure 14: Fault-Free, Full Constellation Availability: Dual Frequency, Fixed Implementation

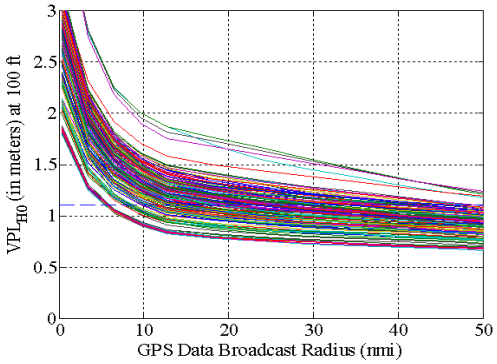

Figure 15: Full Day Results: Single Frequency Floating Implementation

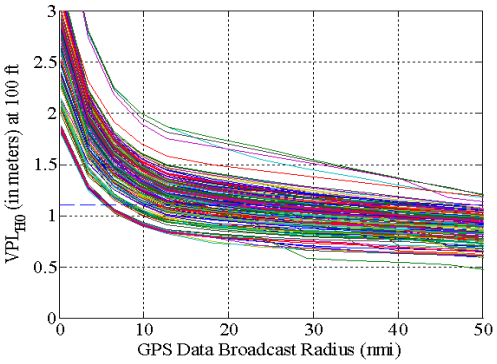

Figure 16: Full Day Results: Single Frequency Fixed Implementation

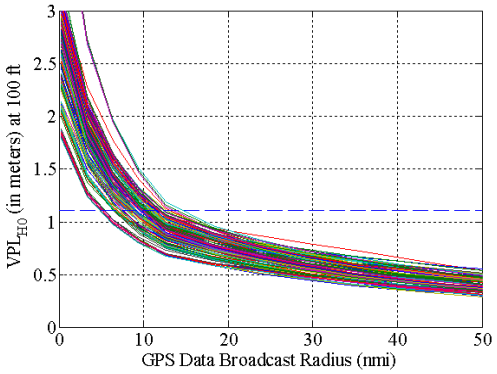

Figure 17: Results with No Ionosphere: Single Frequency Floating Implementation

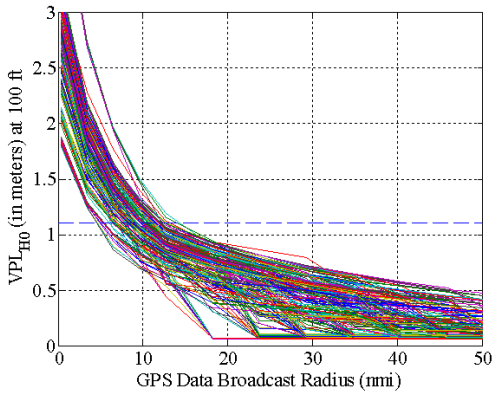

Figure 18: Results with No Ionosphere: Single Frequency Fixed Implementation

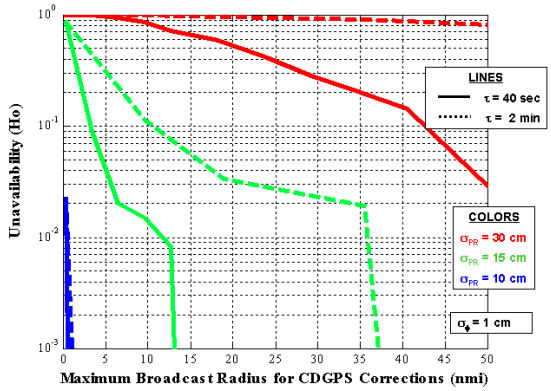

Figure 19: Fault-Free, Full Constellation Availability: Single Frequency, Fixed Implementation

$< 10^{-8}$, VPL_{H0} for the floating implementation is typically already below *VAL*.

Figure 19 shows single-frequency, full-constellation unavailability results (with the nominal ionospheric error model restored) for values of σ_{PR} equal to 10, 15, and 30 cm and measurement error time constants of 40 sec and 2 min. Qualitatively, these results are similar to those from the dual frequency case. As σ_{PR} is lowered, performance is improved and sensitivity to measurement error time constant, and ionospheric/tropospheric model error is effectively reduced. Quantitatively, however, a smaller σ_{PR} —less than approximately 10-12 cm— is required here to achieve results comparable to a dual frequency implementation. Again, as with the dual frequency case, a more stringent requirement will result when satellite outages are considered.

FUTURE WORK: PERFORMANCE IN THE PRESENCE OF FAULTS

The results of this work have so far assumed a full GPS constellation. Analysis of SRGPS availability results with depleted GPS constellations is currently in progress. Similarly, the analysis thus far has assumed that the JPALS system is operating nominally—that is, no failures exist in either the space or shipboard segments. Faults will degrade the performance of the system and, in some instances, lead to hazardous conditions. Thus, during the operation of JPALS such faults have to be detected, alarmed and isolated as soon as possible.

In the JPALS system architecture currently being considered, the task of detecting, alarming and isolating

Monitor	Targeted Fault Mode	Relative Importance to JPALS	Ship Motion Sensitivity	Antenna Motion Sensitivity	Impact of Shipboard Environment
SQM	Signal Deformation	Moderate	Very Small	Moderate	High
Signal Power	RFI, Multipath, Low SV Signal Power	High	Very Small	Small	High
DQM	Navigation Data	Moderate	Very Small	Very Small	None
MQM Carrier	SV clock/RFI/RR tracking	High	High	High	Moderate
MQM Innovation	SV code/RR code tracking	Moderate	Moderate	Moderate	Moderate
B-Value MRCC	Single-RR Failures	High	Very Small	High	Moderate
μ / σ Monitor	Error dist. Change	Moderate	Very Small	High	Moderate
MFRT	Ephemeris errors	Moderate	Moderate	Small	Moderate

Table 1. Summary of the Postulated Effect of GPS Antenna Motion and the Shipboard Enviroment on the JSIM Monitors

space and shipboard segment faults is the responsibility of the JPALS Shipboard Integrity Monitor (JSIM). This system is a shipboard analog of the LAAS Ground Facility (LGF) which is being used as a starting point for the design of the JSIM. There are sufficient differences, however, between the types of operations supported by JPALS and LAAS making a simple transfer of system architecture from the LGF to JSIM not practical.

Firstly, JPALS is fundamentally a carrier-phase system whereas LAAS is a code-phase system. Therefore, in addition to its fault monitoring functions, the JSIM will be responsible for generating and broadcasting high quality carrier- *and* code-phase corrections from *multiple* GPS frequencies to the user.

Secondly, the JSIM is not a static system and will undergo rigid body motion. In addition, due to ship and structural flexing, the various GPS antennas that are part of the system will undergo additional relative motion with respect to each other. Among the important assumptions used in the LGF fault-detection algorithms, however, are that the ground-based reference antennas are rigidly fixed to the earth at surveyed locations, and that the relative baseline vectors between antennas are constant and known very precisely (centimeter level). Since these assumptions are not valid for JSIM, the effect of uncompensated antenna motion on the protection limits must be evaluated. Table 1 lists the LGF integrity monitors which are described in detail in [9], [10] and [11]. Included in Table 1, is the postulated impact of ship and relative antenna motion on these integrity monitors.

Finally, unlike the LGF, the JSIM must operate in a potentially severe multipath and RFI environment. This environment places constraints on where the reference antennas can be located. Extremely tight constraints can ultimately lead to a situation where the multipath seen by all the reference antennas is correlated. Furthermore, since JPALS is a military system, it must be designed such that it continues functioning in an environment where intentional and malicious RFI is present. Clearly, the effects of multipath and RFI must considered when designing the JSIM monitors. The final column of Table 1 ("Impact of Shipboard Environment") includes the postulated impact of multipath and RFI.

CONCLUSIONS

In this paper we explored the sensitivity of fault-free SRGPS performance to data broadcast radius and relevant error parameters including raw code (pseudorange) and carrier measurement error, measurement error time constant, ionospheric spatial gradient uncertainty, and residual tropospheric decorrelation. The results showed that while all parameters affect SRGPS performance, raw pseudorange error is a primary driving parameter if a small (< 10 nmi) data broadcast radius is desired for both fixed and floating implementations. For fixed integer implementations or if a large *DBR* is available, required pseudorange error performance can be traded against carrier phase error performance. In this case, however, robustness to multipath, ionospheric, and tropospheric error model assumptions must be analyzed in greater detail; such an analysis is planned for our continuing work.

In addition, we have shown that the greater sensitivity exhibited by single frequency SRGPS architectures to ionospheric gradient ultimately will result in more stringent requirements on pseudorange measurement error. In addition it was shown that, for the single frequency case, little availability benefit is derived from the use of fixed-integer implementations (relative to floating implementation). This result is in sharp contrast with the dual frequency case, where significant improvement in SRGPS availability can be realized using a fixed-integer implementation. Analysis of SRGPS availability results with depleted GPS constellations is currently in progress.

Finally, we have discussed the issues that have to be addressed when adopting the LGF integrity monitors for shipboard use in the JSIM. Analysis to precisely quantify the effect of ship and antenna relative motion as well as multipath and RFI on these monitors is ongoing. In addition, the use of inertial sensors to detect and compensate for antenna relative motion is being investigated.

ACKNOWLEDGMENTS

The constructive comments and advice regarding this work provided by Frank Allen, John Clark, Ian Gallimore, Glenn Colby, Dennis King, Marie Lage, and Ken Wallace are greatly appreciated. The authors gratefully acknowledge the U.S. Navy (Naval Air Warfare Center) for supporting this research. However, the views expressed in this paper belong to the authors alone and do not necessarily represent the position of any other organization or person.

REFERENCES

[1] JPALS Test Planning Working Group, *Architecture and Requirements Definition: Test and Evaluation Master Plan for JPALS*, January 19, 1999.

[2] A. Brown and N. Gerein, "Test Results from a Digital P(Y) Code Beamsteering Receiver for Multipath Minimization," *Proceedings of the ION 57th Annual Meeting*, Albuquerque, NM, June 11-13, 2001.

[3] G. Colby, "JPALS Navy Program and Requirements Overview," Briefing to SRGPS Architecture Integrated Product Team, March 6, 2001.

[4] K. Wallace, Personal Communication, Aug. 13, 2001.

[5] RTCA SC-159, *Minimum Operational Performance Standards for Global Positioning System/Wide Area Augmentation System Airborne Equipment* (RTCA/DO-229B), Washington, D.C., Oct. 6, 1999.

[6] J. Waters, P. Sousa, L. Wellons, G. Colby, and J. Weir, "Test Results of an F/A-18 Automatic Carrier Landing Using Shipboard Relative GPS," *Proceedings of the ION 57th Annual Meeting*, Albuquerque, NM, June 11-13, 2001.

[7] G. McGraw, T. Murphy, M. Brenner, S. Pullen, and A. J. Van Dierendonck, "Development of the LAAS Accuracy Models," *Proceedings of ION GPS-2000*, Salt Lake City, UT, Sept. 19-22, 2000.

[8] P. Teunissen, D. Odijk, and P. Joosten, "A Probabilistic Evaluation of Correct GPS Ambiguity Resolution," *Proceedings of ION GPS-98*, Nashville, TN, Sept. 15-18, 1998.

[9] G. Xie, S. Pullen, M. Luo, *et.al*., "Integrity Design and Update for the Stanford LAAS Integrity Monitor Testbed," *Proceedings of the 57th ION Annual Meeting*, Albuquerque, NM, June 11-13, 2001.

[10] S. Pullen, M. Luo, S. Gleason, *et. al*., "GBAS Validation Methodology and Test Results from the Stanford LAAS Integrity Testbed," *Proceedings of ION GPS-2000*, Salt Lake City, UT, Sept. 19-22, 2000.

[11] M. Luo, S. Pullen, J. Zhang, *et. al*.,"Development and Testing of the Stanford LAAS Ground Facility Prototype," *Proceedings of ION NTM-2000*, Anaheim, CA, Jan. 26-28, 2000.